J. Membrane Biol. 173, 31–37 (2000)

The Journal of
Membrane
Biology

© Springer-Verlag New York Inc. 2000

Current Oscillations Under Voltage-Clamp Conditions: An Interplay of Series Resistance and Negative Slope Conductance

H. Miedema, E. Balderas, O. Pantoja

Departamento de Biología Molecular de Plantas, Instituto de Biotecnología, Universidad Nacional Autónoma de México, A.P. 510-3, Colonia Miraval, Cuernavaca, Morelos 62250, México

Received: 30 April 1999/Revised: 9 September

Abstract. Using the patch-clamp technique, we observed profound oscillations of the whole-vacuole outward current across the tonoplast of *Mesembryanthemum crystallinum L.* (common ice plant). These current oscillations showed a clear voltage dependence and appeared at membrane potentials more positive than 90–100 mV. This paper describes the oscillations in terms of two separate mechanisms. First, the *Mesembryanthemum* vacuolar membrane shows a negative slope conductance at membrane potentials more positive than 100–120 mV. The fact that the oscillations and the negative slope conductance show a similar threshold potential suggests that (part of) the same mechanism is involved in both phenomena. The second mechanism involved is the voltage drop across the series resistance. As a result, the potential actually experienced by the vacuolar membrane deviates from the command potential defined by the patch-clamp amplifier. This deviation depends in an Ohmic manner on the current magnitude. We suggest that the interplay of the negative slope conductance and the voltage drop across the series resistance can cause a positive feedback which is responsible for the current oscillations.

Key words: Current oscillations — Negative slope conductance — Series resistance — Tonoplast — *Mesembryanthemum crystallinum*

Introduction

In this communication we want to address current oscillations under voltage-clamp conditions as observed in isolated vacuoles of *Mesembryanthemum crystallinum L.*, the common ice plant. We learned that similar oscillations as described here were seen by others also using *Mesembryanthemum* vacuoles (F. Wissing and J.A.C. Smith, *personal communication*). In addition, some kind of oscillatory behavior of whole-vacuole current has been recorded in sugar beet vacuoles (A. Kurkdjian, B. Schulz-Lessdorf and R. Hedrich, *personal communication*). Our experience is that although some colleagues 'intuitively' feel that the access or series resistance (R_s) is involved, nobody really seems to understand these oscillations. At first sight, the view that a changing R_s is responsible for the oscillations may seem plausible. Assume we voltage clamp a membrane containing a conductance that is activated at hyperpolarized potentials. Now, suppose that after the inward current reached steady-state, R_s increases. The result will be a decrease in current, first, because of the voltage drop across R_s the membrane potential (V_m) becomes less negative thereby deactivating channels and, secondly, because of the decrease of V_m, the driving force for ion flow also decreases. When R_s decreases again, the events occur in the opposite direction. The overall result is, indeed, an oscillating current level. Our main objection against such a view is, however, can it really be considered an explanation? The problem is, what causes R_s to change so periodically? Only after one is able to give a satisfying answer to that question, does such a scenario deserve a more serious consideration.

The present study is an attempt to offer an alternative explanation for the oscillatory current behavior. As we will see, we do agree that R_s is involved in this phenomenon, but not in the way pictured above. Instead, this study can be considered as an extension of the early work of Cole and Moore (1960) and of Armstrong and Gilly (1992) and Marty and Neher (1995). These studies

Correspondence to: O. Pantoja

address effects of R_s on the voltage-clamp and current response. Although oscillations of V_m in plant cells have been reported frequently, for instance in connection with oscillations of the cytosolic Ca^{2+} level (Grabov & Blatt, 1998), to our knowledge this is the first study to report current oscillations. Although the precise underlying mechanism for oscillations of V_m and current may be quite distinct, we argue that part of the same mechanism that is involved in the oscillations of V_m also plays an important role in the oscillations of whole-vacuole current described here.

Material and Methods

Plant Material

Mesembryanthemum crystallinum L. was grown as described previously (Barkla et al., 1999). Leaf mesophyll protoplasts were obtained by enzymatic digestion. After stripping off the epidermis at the abaxial side and the removal of the major veins, the leaf was cut into small pices and incubated for 45 min at 30°C in an enzyme solution containing 0.05% cellulase RS (Onozuka, Japan), 0.01% pectolyase Y-23 (Seishin, Japan) and 1% BSA (Sigma, Mexico). After pipetting off the enzyme solution, 10 ml of patch-clamp bath solution was added. Protoplasts were released by gently shaking the petri dish. Protoplast yield was significantly improved by pulling the leaf slowly over the edge of the petri dish. The protoplast containing solution was pipetted into a test tube and protoplasts were collected by sedimentation. Approximately 8 ml of the solution was pipetted off and the protoplasts were kept on ice in the remaining 2 ml bath solution. Vacuoles were obtained by osmotic shock, using a 100 mM EGTA solution, adjusted with Tris to pH 7, resulting in a final osmolality of 200 mmol kg^{-1}. To 0.3 ml of protoplast solution, 0.9 ml of EGTA solution was added and protoplast lysis was followed under the microscope. When approximately 50% of the vacuoles were released (typically after 3–5 min), lysis was stopped by adding 5 ml bath solution. After the vacuoles had sedimented to the bottom of the dish, the vacuoles were washed three times with 5 ml bath solution. The vacuoles used for the patch-clamp experiments typically had a diameter of 100 μm.

Patch Clamp

Patch-clamp recording and data analysis were performed using an Axopatch 200B amplifier, a 1200 Digidata interface and pClamp 6.0.4. software (Axon Instruments, Foster City, CA). Whole-vacuole and excised-patch data were sampled at 2 and 5 kHz, respectively, and the data were filtered at a −3 dB frequency of 1 kHz using the electronics on the Axopatch amplifier. Series resistance compensation appeared to be extremely difficult for these vacuoles, possibly due to the large current magnitudes observed. For that reason and because overcompensation itself may even lead to oscillations ('ringing'), we did not apply series resistance compensation. Pipettes were pulled from glass capillaries (Sigma, Mexico, # P-1174), using a two-stage pipette puller (Narishige, Tokyo, # PP-83).

Unless stated otherwise, the composition of the pipette solution was (in mM): 10 K_2Malate, 1 $CaCl_2$, 10 MES, pH 5.5. The bath solution contained: 100 K_2Malate, 1 $CaCl_2$, 10 HEPES, pH 7.5. To both pipette and bath solution sorbitol was added to a final osmolality of 500 mmol kg^{-1}. Instead of using rather expensive K_2Malate, H_2Malate solutions were titrated with KOH to the desired pH. Ion activities were calculated with Geochem-PC 2.0 (Parker, Norvell & Chaney, 1995) and the free Ca^{2+} activities in the pipette and bath solution were 308 and 85 μM, respectively. The calculated Nernst potentials were (in mV): −53 for K^+, 25 for $Malate^{2-}$, −5 for Cl^- and 16 for Ca^{2+}. The reference electrode was connected to the bath solution via a 2.5 M KCl/1% agar bridge. Liquid junction potentials (LJP) were measured according to the protocol outlined by Ward and Schroeder (1994) and this procedure resulted in a LJP of −10 mV, the pipette positive because the bath contained an excess of K_2Malate, and K^+ has the larger mobility coefficient. We followed the current and voltage convention proposed by Bertl et al. (1992). This implies that in the whole-vacuole and outside-out patch configuration a flux of cations into the vacuolar lumen is assigned as positive current. It should be stressed that according to this convention a positive current is thus defined as a flux of cations into the pipette, i.e., the opposite direction as defined by the Axopatch 200B amplifier. Similarly, in the whole-vacuole and outside-out patch configuration, V_m equals the negative of the applied pipette potential (V_p): $V_m = -V_p$. When LJP is defined as the potential of the bath solution with respect to the pipette solution, V_m equals the difference between LJP and the potential read from the amplifier's display (V) (Neher, 1992):

$$V_m = -V_P = LJP - V \quad (1)$$

Throughout the text, membrane potentials have been corrected for LJP.

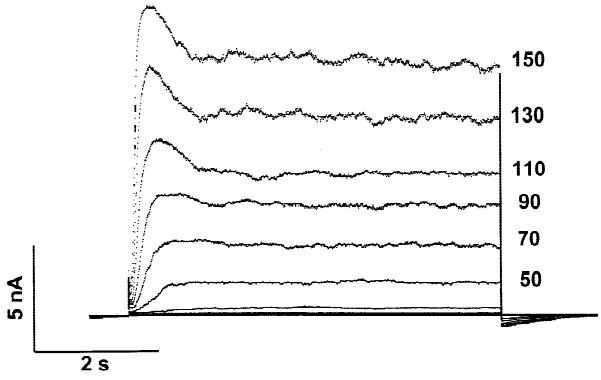

Fig. 1. Activation of outward current during a whole-vacuole recording in response to membrane potentials (V_m) ranging from 10 to 150 mV, in 20 mV steps and starting from a holding potential of −10 mV. Note the appearance of the shoulder at V_m more positive than 90 mV. Currents were recorded in 10/100 mM (vacuolar/cytosolic) K_2Malate solutions.

Results

With 10 mM K_2Malate in the pipette and 100 mM K_2Malate in the bath solution, membrane potentials more positive than 20 to 40 mV evoked two different types of responses in the *Mesembryanthemum* vacuole. An example of the first type is given in Fig. 1, which presents current recordings in the whole-vacuole configuration in response to V_m ranging from 10 to 150 mV, in 20 mV steps and starting from a holding potential of −10 mV. Notable is the typical shoulder in the current traces at V_m more positive than 90 mV. Figure 2 shows an ex-

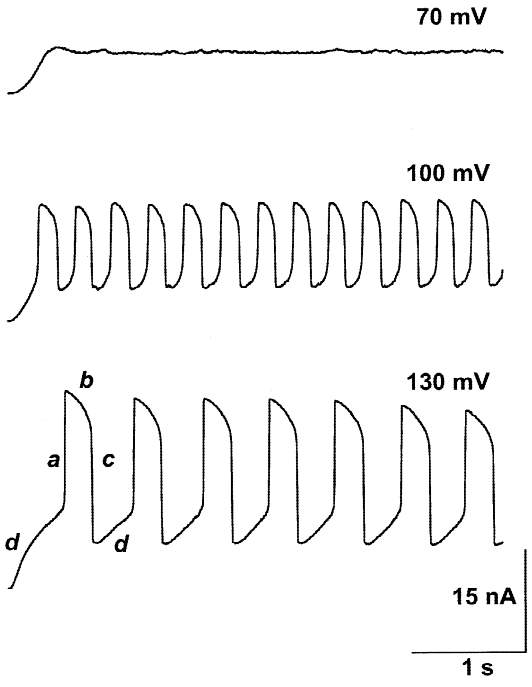

Fig. 2. Current oscillations in a vacuole exposed to a similar pulse protocol and to identical ionic conditions as employed in Fig. 1. At V_m more positive than 90—100 mV, the whole-vacuolar current started to oscillate and two examples at 100 and 130 mV are shown. Note the voltage dependence of the frequency of these oscillations: the more positive V_m, the lower the frequency. In the bottom trace, the four distinct phases of a single oscillation are marked with *a* through *d* (*see text*). For reasons of clarity, the data points are interconnected.

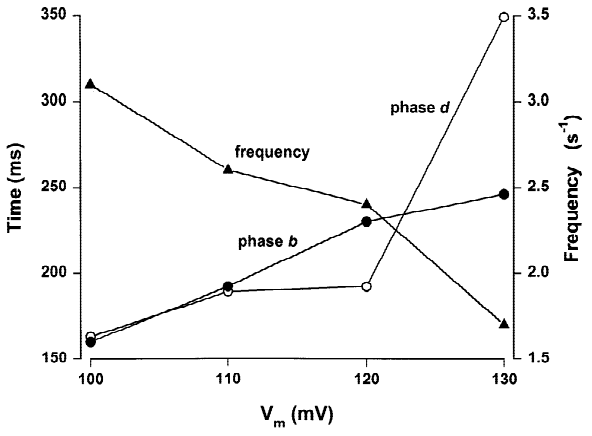

Fig. 3. Voltage dependence of the oscillations shown in Fig. 2. The duration of phases *b* and *d* (*see* bottom trace Fig. 2) are plotted as a function of V_m. Note that, because of the voltage sensitivity of phases *b* and *d*, the frequency of the oscillations, defined as $1/(b + d)$, decreases at more positive V_m.

ample of the second type of response. A similar pulse protocol to that used in Fig. 1 elicited an outward current of comparable magnitude. However, in this case the whole-vacuole current started to oscillate, typically at V_m more positive than 90–100 mV, i.e., the same threshold potential as for the shoulder to appear in the non-oscillating current in Fig. 1. This similarity suggests that the same mechanism is responsible for, or at least involved in, the two different current responses. The time course of one complete oscillation can be dissected into four distinct phases, in the bottom trace of Fig. 2 designated by *a* through *d:* a first, almost instantaneous transition of current to a more positive level (*a*), a second, relatively slow relaxation to a slightly less positive current level (*b*), a third, fast transition in current level, kinetically similar to the *a*-phase but in the opposite direction (*c*) and, finally, a fourth phase, also relatively slow and to a more positive level (*d*). The voltage dependence of the oscillations is not only reflected in the threshold potential of 90 mV mentioned above, but also in a frequency that decreased at more positive V_m. This voltage dependence is presented in Fig. 3. Both the duration of the oscillations, i.e., phase *b* in Fig. 2, and the time in between the oscillations, i.e., phase *d* in Fig. 2, increased at more positive V_m. As a result the frequency of the oscillations decreased at more positive V_m. The effect of V_m on the oscillations is also obvious from Fig. 4 which shows a nonoscillating current at a V_m of 110 mV that, upon a depolarization as small as 10 mV, started to oscillate instantaneously.

The first step in the understanding of the oscillations arose from the realization that during a voltage-clamp measurement, V_m is not clamped at exactly V_p. The reason is that the membrane resistance (R_m) and the series resistance (R_s) are positioned in a voltage divider. According to Ohm's law, the voltage drop across R_s is proportional to R_s and the current (I) that flows through R_s. Consequently, although during a 'voltage-clamp' recording V_m is indeed under control of the patch-clamp amplifier, the potential actually experienced by the membrane, i.e., V_m, deviates from V_p by IR_s. In the case of the whole-cell configuration in which V_m equals V_p, a flux of cations into the pipette ($I < 0$) depolarizes V_m (Armstrong & Gilly, 1992). According to the sign convention used here, this implies for vacuoles an effect in the opposite direction: V_m deviates from $-V_p$ and a flux of cations into the pipette ($I > 0$) hyperpolarizes V_m, i.e., moves V_m into the negative direction away from $-V_p$ and vice versa in the case of inward current. Therefore, instead of Eq. 1, it is more appropriate to define V_m as:

$$V_m = LJP - V - IR_s = -V_p - IR_s \qquad (2)$$

It should be noted that because of this R_s-effect, during the recording shown in Fig. 2, V_m oscillated as well with a frequency that, according to Eq. 2, exactly mirrored the frequency of the current oscillations.

The second step towards understanding the current oscillations came from the use of voltage ramp protocols.

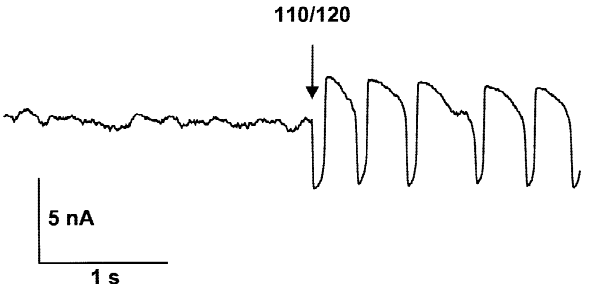

Fig. 4. Response of a whole-vacuole current to a depolarizing pulse of 10 mV. Prior to the voltage pulse to a V_m of 120 mV, the outward current was activated to a steady-state level by clamping the vacuole at a V_m of 110 mV. Ionic conditions were as in Fig. 1. For reasons of clarity, the data points are interconnected.

Figure 5 shows current recordings of an outside-out patch in response to a ramp protocol from a V_m of −10 mV to either 70, 110, 150 or 190 mV, followed by a ramp back to −10 mV. In all cases, the speed of the ramp, expressed as voltage change per unit time, was the same: 100 mV in 3.5 sec, i.e., 28.6 mV/sec. The ramp recordings of Fig. 5 were transformed into current-voltage relationships (*IV*-plots) and these *IV*-plots are shown in Fig. 6. Each curve in Fig. 6 is based on the average of 10 consecutive recordings as shown in Fig. 5. The *IV*-plot derived from a ramp from −10 to 70 mV (Fig. 6*A*) coincides with the one in the opposite direction, i.e., from 70 to −10 mV. This means that in this voltage range the membrane slope-conductance, i.e., the tangent at each point of the curve in Fig. 6*A*, is independent of the direction of the voltage change. This conclusion, however, does not hold at more positive potentials. During a polarization of the membrane from −10 to 110 mV (Fig. 6*B*), 150 mV (Fig. 6*C*) or 190 mV (Fig. 6*D*), the membrane also shows a positive slope conductance. This reflects nothing but Ohm's law: an increase in driving force correlates with an increase of outward current. But this is not true when the ramp is applied in the opposite direction. Starting from a potential more positive than 70 mV, a change of potential in the negative direction causes a temporal increase in outward current. The threshold voltage for the negative slope conductance appears to fall in the same range as the threshold potential of 90 mV found for the shoulder in Fig. 1 and the oscillations in Fig. 2. This similarity in voltage sensitivity suggests that the same underlying mechanism is involved in these three phenomena. A negative slope conductance implies an increase of outward current with decreasing potential, i.e., a current increase despite a decrease of driving force. Obviously, the gating kinetics of the channel that mediates the outward current must be responsible for this effect. Apparently, changing the potential from, for instance, 140 to 100 mV causes a temporal increase in the number of activated channels. As a result, despite the decline in driving force, the net effect

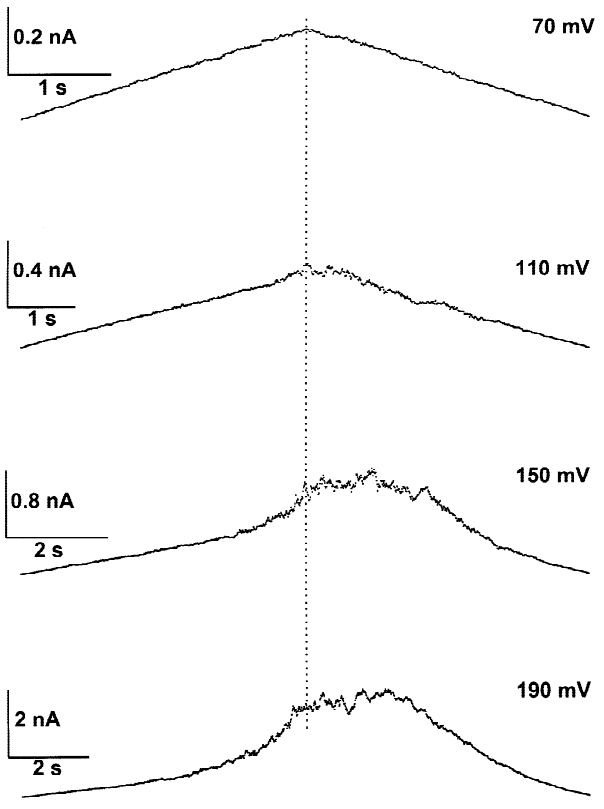

Fig. 5. Current response in an outside-out patch to a voltage ramp protocol from a holding potential of −10 mV to either a V_m of 70, 110, 150 or 190 mV, and in all cases back to −10 mV. The speed of the ramp (28.6 mV/sec) was the same for all four ramps which is reflected in the time scale bars belonging to each trace. The dotted, vertical line indicates the turning point of the voltage ramp. Ionic conditions were as in Fig. 1.

is an increase in current magnitude. Similar *IV*-plots showing a negative slope conductance were obtained from ramp protocols imposed on whole-vacuoles (*result not shown*). Although the voltage ramps in Fig. 5 were applied at a rather slow speed (100 mV in 3.5 sec), one may argue that the negative slope conductance reflects a time effect rather than an effect of voltage: after the ramp reverses direction channels continue to open and as a net result the slope conductance increases. For that reason, we also investigated the conductive behavior as determined from steady-state current levels. As outlined above, due to the effect introduced by R_s, V_m deviates in an Ohmic manner from $-V_p$. Therefore, in order to limit this R_s-effect as much as possible, we studied the conductive behavior of the *Mesembryanthemum* tonoplast in outside-out patches. Because of the lower current magnitude in the excised patch the voltage drop across R_s will be proportionally smaller. An example of such a recording in symmetrical 10 mM K_2 Malate solutions is shown in Fig. 7*A*. The current traces overlapped and for reasons of clarity only the traces recorded at 80, 160 and

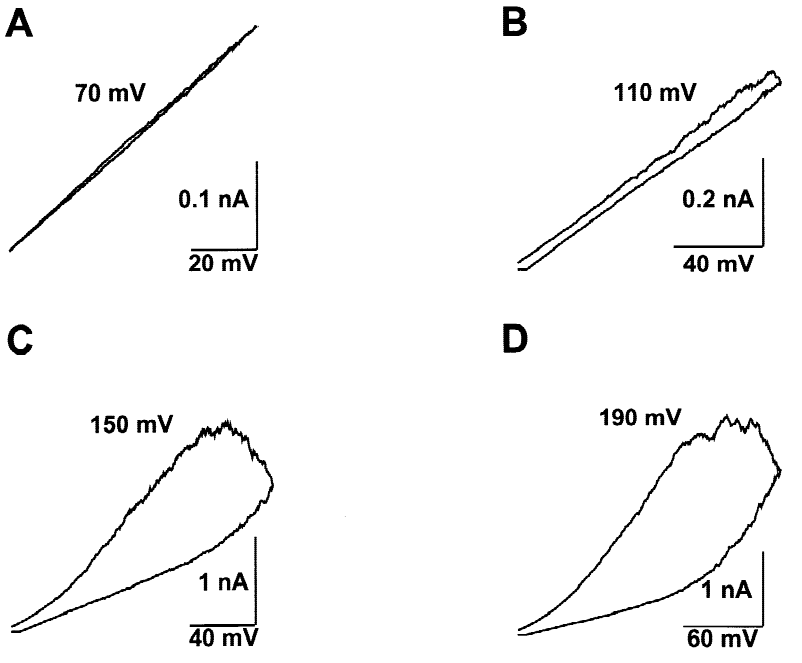

Fig. 6. Current-voltage relationships (*IV*-plots) belonging to the data shown in Fig. 5. *IV*-plots were derived from average traces of 10 consecutive recordings as shown in Fig. 5. Note, the negative slope conductance in the *IV*-plots of 110, 150 and 190 mV but not in the one of 70 mV.

190 mV are shown. The negative chord conductance derived from the steady-state current levels (I_{ss}) already emerges from this figure. Figure 7*B* shows normalized conductances (G/G_{max}) calculated over the entire voltage range tested (0 to 200 mV). Because of zero E_{rev}, the chord conductance (G) is given by I_{ss}/V_m, where I_{ss} was obtained after averaging the current over the last 1.5 sec. To obtain G_{max}, in the voltage range in which G showed the typical S-shaped dependence on V_m (0 to 120 mV), G was fitted as a function of V_m to a Boltzmann-like expression. Finally, over the entire voltage range, G values were divided by G_{max}. The result is shown in Fig. 7*B* and the negative slope conductance at V_ms more positive than 120 mV falls in the same range as the negative slope conductance observed when applying a voltage ramp protocol (Figs. 5 and 6). From Fig. 7*B* we conclude that the negative slope conductance in Fig. 6 indeed reflects an effect due to voltage and not to time.

Given the finding of the negative slope conductance and the realization of the effect of R_s on the voltage clamp, we return to the oscillations. The combination of the negative slope conductance and the voltage drop across R_s can create a positive feedback. Suppose we pulse from a holding potential of zero mV to, for instance, 180 mV. Initially, all channels are closed and $V_m = -V_p$. Upon polarization, outward current starts to flow. As outward current develops, V_m moves in the negative direction away from $-V_p$, according to Eq. 2. But then, given the negative slope conductance of the vacuolar membrane, this causes more channels to open. This, in turn, allows more current to flow, which moves V_m even further away from $-V_p$. This snowball effect is halted for two reasons. First, V_m moves to a voltage

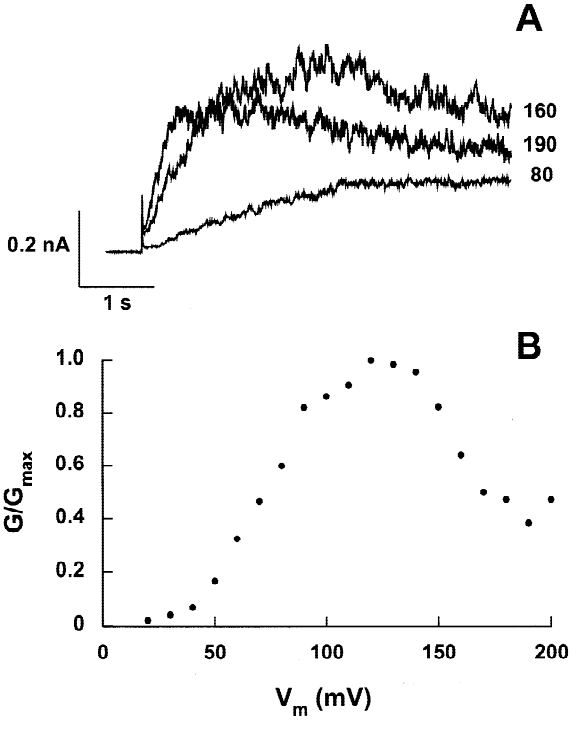

Fig. 7. (*A*) Current recordings on an outside-out patch, starting from a zero holding potential. Values of V_m are indicated on the right hand side of the traces. Because the traces overlapped, only the traces at 80, 160 and 190 mV are shown. Pipette and bath solution both contained 10 mM K_2Malate. (*B*) Normalized conductances (G/G_{max}) as a function of V_m. Note the negative chord conductance at potentials more positive than 120 mV.

range where the *IV*-plot starts to bend in the opposite direction, i.e., to a voltage at which the membrane starts to show a positive slope conductance. At that point, the positive feedback is turned into a negative feedback: as V_m moves in the negative direction away from $-V_p$, channels start to deactivate, thereby decreasing the outward current magnitude, which, in turn, causes V_m to move back in the direction of $-V_p$. Secondly, the transition in current level towards more positive values causes V_m to hyperpolarize and, eventually, channels to deactivate. Note that, according to Eq. 2, the combination of an outward current of 10 nA and an R_s of 5 MΩ hyperpolarizes V_m by not less than 50 mV and this number further increases to 100 mV in the case of an R_s of 10 MΩ. Once the hyperpolarization of V_m has been initialized the very same mechanism can create a positive feedback again, but now occurring in the opposite direction: channels deactivate, thereby lowering the current magnitude. Because of this, V_m moves into the direction of $-V_p$, causing even more channels to deactivate, resulting in less current flowing despite the increase in driving force, and so on. When most of the channels are closed, the outward current has been dropped to a level close to zero pA. Consequently, the deviation of V_m from $-V_p$ subsides and the amplifier clamps the membrane again at $-V_p$ and the cycle can start all over again.

Discussion

The effects of R_s on the quality of the voltage clamp have been recognized for a long time. Already 40 years ago, effects associated with R_s were discussed by Cole and Moore (1960). Later, the issue was addressed extensively by Armstrong and Gilly (1992) and Marty and Neher (1995). These studies outline a scenario based on the combination of a negative slope conductance and R_s. Armstrong and Gilly (1992) simulate the current response in the case of a low and high R_s. They elegantly demonstrate that a high R_s and a negative slope conductance may result in an almost instantaneous transition of current and membrane potential and in that context they refer to an action potential. Similar conclusions can be found in Marty and Neher (1995) as they state that in the case of $dI/dt < 0$, 'total voltage clamp failure can occur'. In this respect, our observations are in good agreement with the conclusions reached in these more theoretical papers, in particularly as the very fast, almost instantaneous transitions in current level during phases *a* and *c* of an oscillation are concerned (Fig. 2). The current oscillations discussed here demonstrate to what kind of response the combined effects of R_s and a negative slope conductance ultimately may lead. Although neither Armstrong and Gilly (1992) nor Marty and Neher (1995) refer to the possibility of current oscillations, we believe that this oscillatory behavior is essentially based on the same principle. Because V_m is totally out of control, after phase *a* has been completed, V_m has been hyperpolarized. As a consequence, channels start to deactivate. Once the deactivation has been initialized, the very same positive feedback occurs in the opposite direction and accounts for the almost instantaneous current transition during phase *c*. It should be realized that both a V_m that changes because of the R_s-effect and a negative slope conductance are necessary to induce the positive feedback. In the hypothetical case of zero R_s, there is no voltage drop across R_s and despite the negative slope conductance V_m remains clamped at exactly $-V_p$. On the other hand, activation at a potential at which the membrane shows a positive slope conductance will result in a negative feedback: as outward current develops, V_m moves away from $-V_p$ to a less positive value causing channels to deactivate instead of activate. The current magnitude reduces and so does the voltage drop across R_s. As a consequence, V_m moves back in the direction of $-V_p$.

Although the effect of R_s is always present, there are several ways to limit the interference of R_s on the recording as much as possible. The first thing to do is to pull low-resistence patch-clamp pipettes. Secondly, in order to reduce the current magnitude, and thus the voltage drop across R_s, one can select small cells or vacuoles. In case of *Mesembryanthemum* this is however hardly a solution. Even relatively small vacuoles still have a diameter of tens of μm. In addition, as mentioned before, probably because of the high current magnitudes, series compensation appeared extremely difficult during recordings on *Mesembryanthemum.* But even if series compensation is quite feasible, one should keep in mind that a 100% compensation is impossible and that typically 5–10% remains uncompensated. To reduce the current magnitude one may choose the use of low ionic solutions. It should be realized however that a low ionic pipette solution will increase R_s. In this respect, we have one additional argument that R_s is indeed involved in the current oscillations described here. The value of the pipette resistence (R_{pip}) as measured before sealing the pipette at the membrane surface strongly depends on the pipette solution used. With 10 mM K_2 Malate in the pipette, R_{pip} typically was 16–18 MΩ. Increasing the amount of K_2 Malate in the pipette to 100 mM lowered R_{pip} tenfold. As a rule of thumb, R_s will be at least twice as great as R_{pip} (Marty & Neher, 1995). As a consequence, when using the 10 mM K_2 Malate pipette solution, R_s was at least ten times higher than when using the 100 mM K_2 Malate solution. This consideration may explain why oscillations were observed almost exclusively with 10 mM K_2 Malate in the pipette solution.

In vivo, the vacuolar membrane is exposed to a free-running V_m. As outlined by Buschmann and Gradmann

(1997), one of the prerequisites for the oscillations of V_m to occur is the involvement of a channel that demonstrates a negative slope conductance. In this respect, the oscillations of V_m and the current oscillations described here have in common part of the mechanism responsible for the two types of oscillation as they both require a positive feedback induced by the negative slope conductance. Finally, it should be noted that, by definition, ion channels are only able to dissipate gradients of the chemical potential of ion species across the membrane. Therefore, oscillations of V_m and current oscillations alike need the input of free energy. Obviously, in case of the current oscillations under voltage-clamp, or better, semi-voltage-clamp conditions, the patch-clamp amplifier fullfills this task.

Conclusions

We are very well aware that the explanation for the current oscillations we give does not elucidate all the details. Nevertheless, the mechanism described here can account for the oscillatory current behavior under voltage–clamp conditions, at least at the qualitative level. In that respect, the minimum model proposed, based on the studies of Armstrong and Gilly (1992) and Marty and Neher (1995), is a first step towards a better understanding of this phenomenon. But a number of intriguing questions remain open. Notably, are these oscillations regulated at another level as well? For instance, is it possible to induce oscillations by changing the ionic conditions to which the *Mesembryanthemum* tonoplast is exposed? Why do some vacuoles show the typical shoulder but do not start to oscillate? What does this imply for the coordination of the separate phases of an oscillation? How to explain exactly the voltage dependence of the frequency of the oscillations? These questions, among others, may find an answer in future research.

This study was supported by Grants awarded to O.P. by CONACyT (4745-N) and DGAPA (IN202495).

References

Armstrong, C.M., Gilly, W.F. 1992. Access resistance and space problems associated with whole-cell patch clamping. *Methods in Enzymology* **207:**100–122

Barkla, B.J., Vera-Estrella, R., Maldonado-Gama, M., Pantoja, O. 1999. ABA induction of vacuolar H^+-ATPase activity in *Mesembryanthemum crystallinum L.* is developmentally regulated. *Plant Physiol.* **120:**811–819

Bertl, A., Blumwald E., Coronado, R., Eisenberg, R., Findlay, G., Gradmann, D., Hille, B., Köhler, K., Kolb, H.A., MacRobbie, E., Meissner, G., Miller, C., Neher, E., Palade, P., Pantoja, O., Sanders, D., Schroeder, J., Slayman, C., Spanswick, R., Walker, A., Williams, A. 1992. Electrical measurements on endomembranes. *Science* **258:**873–874

Buschmann, P., Gradmann, D. 1997. Minimal model for oscillations of membrane voltage in plant cells. *J. Theor. Biol.* **188:**323–332

Cole, K.S., Moore, J.W. 1960. Ionic current measurements in the squid giant axon membrane. *J. Gen. Physiol.* **44:**123–167

Grabov, A., Blatt, M.R. 1998. Membrane voltage initiates Ca^{2+} waves and potentiates Ca^{2+} increases with abscisic acid in stomatal guard cells. *Proc. Natl. Acad. Sci. USA* **95:**4778–4783

Marty, A., Neher, E. 1995. Tight-seal whole-cell recording. *In:* Single-channel recording. B. Sakmann and E. Neher, editors. pp. 31–52. Plenum Press, New York

Neher, E. 1992. Correction for liquid junction potentials in patch clamp experiments. *In: Methods in Enzymology* **207:**123–131

Parker, D.R., Norvell, W.A., Chaney, R.L. 1995. GEOCHEM-PC: A chemical speciation program for IBM and compatible personal computers. *In:* Chemical Equilibrium and Reaction Models. R.H. Loeppert, A.P. Schwab and S. Goldberg, editors. pp. 253–269. SSSA Special publication number 42, Soil Science Society of America/American Society of Agronomy, Madison, WC

Ward, J.M., Schroeder, J.I. 1994. Calcium-activated K^+ channels and calcium-induced calcium release by slow vacuolar ion channels in guard cell vacuoles implicated in the control of stomatal closure. *Plant Cell* **6:**669–683